High-performance laser power feedback control system for cold atom physics

Bo Lu (鹿 博), Thibault Vogt, Xinxing Liu (刘新星), Xiaoji Zhou (周小计)*, and Xuzong Chen (陈徐宗)**

School of Electronics Engineering and Computer Science, Peking University, Beijing 100871, China

**Corresponding author: xjzhou@pku.edu.cn; **corresponding author: xuzongchen@pku.edu.cn*

Received February 14, 2011; accepted April 4, 2011; posted online June 21, 2011

A laser power feedback control system that features fast response, large-scale performance, low noise, and excellent stability is presented. Some essential points used for optimization are described. Primary optical lattice experiments are given as examples to show the performance of this system. With these performance characteristics, the power control system is useful for applications in cold atom physics and precision measurements.

OCIS codes: 140.3425, 020.1475, 000.3110.
doi: 10.3788/COL201109.091403.

Neutral atoms in optical lattices have been extensively studied in recent years. The optical lattice clock, in which atoms trapped in an optical lattice serve as quantum references, has demonstrated a promising way toward frequency standards with improved accuracy[1]. Ultracold atoms stored in optical lattices provide outstanding possibilities for implementing designs for quantum information processing[2]. A Bose-Einstein condensate (BEC) loaded in an optical lattice has been studied as a model system for condensed matter phenomena. The quantum phase transition between the superfluid and the Mott insulator phase has been investigated in optical lattices[3,4]. Moreover, various topics about ultracold atoms and optical lattices, such as ferromagnetism[5], spinor systems in optical lattice[6], and disordered systems[7], have been proposed and warrant further studies.

An optical lattice can be obtained when two laser beams with the same wavelength propagating in different directions meet each other and form an interference pattern. In such a lattice, the atoms can be trapped because the electric fields of the lasers induce an electric dipole moment in the atom. The interaction between this dipole moment and the electric field of the laser can generate the optical dipole force[8]. If the laser frequency is less than a specific electronic transition frequency within an atom, the atoms are trapped in the intensity maxima of the light field. In contrast, if the laser frequency is higher than the transition frequency, the atoms are trapped in the intensity minima. Ultracold atoms in optical lattices are versatile tools for cold atomic physicists because they have many advantages over conventional condensed matter systems. Lattice dimensionality can be changed easily. The geometry of the lattices can be altered by interfering laser beams under the different angles, thus making even more discretionary lattice configurations. Optical lattice potentials can even be varied dynamically during an experimental sequence by simply increasing or decreasing the power of the laser[9]. In order to obtain a stable lattice, it is better to stabilize first the laser frequency using saturated absorption spectroscopy or the Pound-Drever-Hall technique[10]. A high-performance power control system then becomes important for optical lattice experiments.

In this letter, we present a laser power control system that combines wide dynamic range, fast response, low noise, and excellent stability. Figure 1 shows the schematic drawing of the power control apparatus for the optical lattice experiments. The ^{87}Rb BEC setup is similar to the one described in our previous studies[11,12]. The extended cavity diode laser (ECDL) centered around 852 nm is similar to that presented in our previous work[13]. The ECDL has an output power of up to 30 mW and can be frequency stabilized for many hours. The laser from the ECDL is amplified by the tapered amplifier (TA) as we reported in Ref. [14]. Using this master oscillator power amplifier (MOPA) system, more than 500 mW of output power can be achieved. A function generator (Agilent Technologies 33220A) is controlled by a LABVIEW program to create a stable, accurate reference signal for power control circuit. An acousto-optical modulator (AOM) is employed as a controllable optical attenuator. The first diffraction-order beam is spatially filtered and guided to the experiment using a polarization-maintaining fiber (PMF). After the fiber coupler, a half-wave plate ($\lambda/2$) is used for rotating the polarization of the laser to pass through a polarizing beamsplitter cube (PBS). The PBS is employed to clean up the polarization of the light. A pick-off glass is used to send a few percentage of the light onto a photodetector (PD). The output of the PD is compared with the

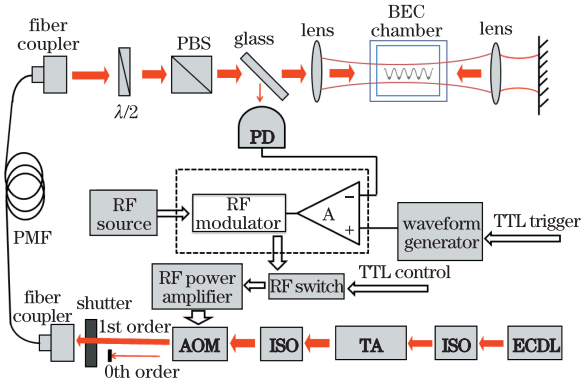

Fig. 1. Schematic drawing of the laser power controller for the optical lattice experiments. ISO: optical isolator.

reference signal to generate the error signal. The radio frequency (RF) modulator is controlled by the error signal via a proportional-integral-derivative (PID) controller. The RF amplifier amplifies the output of the RF modulator via a switch, such that the RF output is sufficient to drive the AOM. The RF switch controlled by an external transistor-transistor logic (TTL) signal is used to rapidly switch on or off the RF signal to the amplifier. The intensity-controlled beam is then focused on the condensate using a lens. The beam is re-collimated after exiting the chamber and is then retro-reflected. The BEC is loaded in this one-dimensional (1D) lattice created by retro-reflecting the injected laser beam.

In optical lattice experiments, the lattice depth should be changed reproducibly. If the output power of the TA or the fiber transmittance fluctuates, the optical potential should be kept constant. Hence, the lattice laser must be locked to the reference signal generated by the function generator. In order to obtain a short response time, we optimized the system in three aspects. Firstly, we used a RF switch as RF modulator, instead of a voltage variable attenuator. Compared with the nearly 25 μs rise and fall time of the variable attenuator, the RF switch has a much faster rise and fall time on the order of 5 ns. We can choose a special RF switch as a modulator, which has a slowly varying control voltage between the low state and the high state. Secondly, we reduced the rise and fall time of the AOM. After applying a RF signal to an AOM, it will generate an acoustic wave. This acts like a phase grating traveling through the crystal at the acoustic velocity of the material. Any incident laser beam will be diffracted by this grating, giving diffracted beams. Thus, there is a delay between turning on the RF signal and generating the first diffraction order due to the finite acoustic velocity (in our case, model AA.MT.110-IR, 4 200 m/s). In order to reduce this delay, we changed the configuration by focusing the injected beam a little bit smaller with two lenses (see Fig. 2(a)). Because the diameter of the beam is smaller, we can align the light to go through at different positions of the AOM aperture. When the beam goes through the center of the AOM aperture (see Fig. 2(b)), the delay is measured to be around 600 ns. If the beam goes through the part close to the edge of the AOM aperture (see Fig. 2(c)), the delay can be reduced to 300 ns. This method can significantly reduce the rise and fall time of the AOM. Thirdly, we employed a high-speed photodetector with a rise time on the order of 10 ns. After optimizing the above apparatus, we obtained a fast servo loop with a response time shorter than 20 μs, which is sufficient for optical lattice experiments. Because the photodetector is accurate and has a large dynamic range, the lattice depth in our experiment can be controlled between 0 and 160 $E_{\rm R}$, where $E_{\rm R} = \hbar^2 k^2/2m$ is the recoil energy.

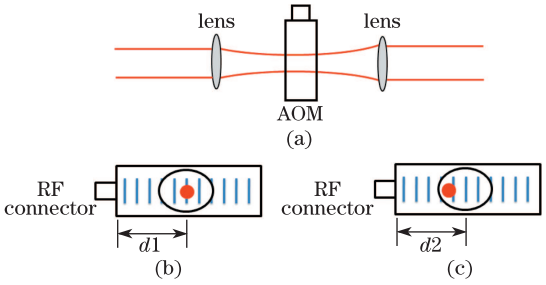

Fig. 2. AOM alignment for short rise and fall time. (a) Two lenses are used to focus and re-collimate a laser beam passing through the AOM. Align laser beams passing through (b) the center and (c) the edge of AOM apertures.

In order to achieve a low noise and excellent stability power control system, we optimized the system in following aspects. Firstly, we used an angle-polished fiber to avoid near-normal reflections off the face of the fiber. The interference signal between the initial and retro-reflected beam can lead to intensity fluctuations. Back reflections can form an interference pattern on the photodetector used to sample the intensity of the beam. The feedback then stabilizes the interference signal between the initial and retro-reflected beam, leading to intensity fluctuations. These intensity fluctuations lead to the heating of atoms in the lattice and shortened lifetime. Using angle-polished fibers can minimize this problem. Secondly, we optimized the time sequence for the AOM. After turning on the RF signal, we found that the AOM needs a few minutes to reach a stable state. Although the response time of the AOM is short, this long warm-up period can affect the reproducibility of experiments and cause intensity fluctuations. In order to solve this problem, we used a mechanical shutter before the AOM. When we need the laser beam to be on, the shutter is opened and the AOM works in a controllable mode. During the gap between two optical lattice laser pulses, the shutter is closed to completely cut off the light and the AOM works in a continuous mode. In this way, the warm-up period of the AOM can be neglected. Thirdly, the whole power control system was designed using analog circuits and needs only two TTL signals as triggers. Using these methods, fluctuations are limited to less than 0.3%. Moreover, we obtained a long atom lifetime inside the optical lattice.

A clear way to demonstrate the performance of the power control system is to load a BEC into an optical lattice. The lattice depth can be calibrated via Kapitza-Dirac scattering[15,16]. If a BEC is adiabatically loaded into an optical lattice by slowly ramping up the optical lattice potential, the wave function of the condensate

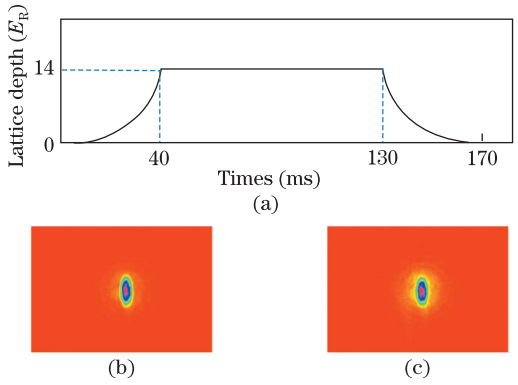

Fig. 3. Measurement for reversible loading of a BEC in optical lattices. (a) Experimental sequence used for adiabatically loading the BEC into an optical lattice in 40 ms with a time constant of 20 ms. After a hold time of 90 ms, the lattice potential is ramped down to 0 $E_{\rm R}$; (b) absorption image of a BEC after 30-ms time of flight; (c) absorption image of a BEC undergoing the process of reversible loading in optical lattices.

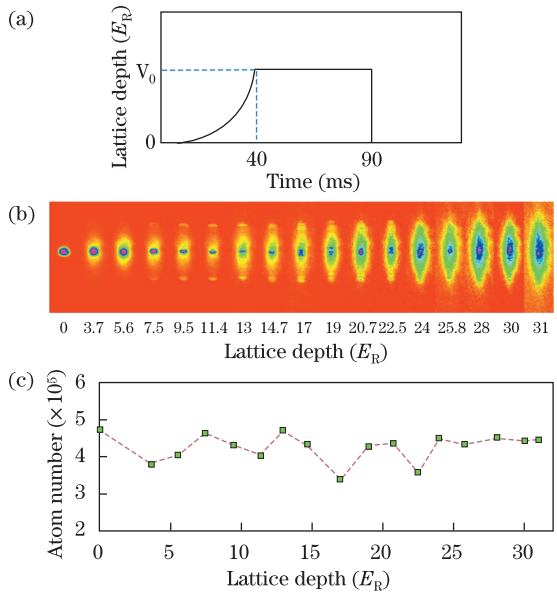

Fig. 4. Experiments to observe trap states from superfluidity to number squeezed state. (a) Experimental sequence used for adiabatically loading the BEC into an optical lattice in 40 ms with a time constant of 20 ms. The atoms are held at different lattice depths (from 0 E_R to 31 E_R) for 50 ms and the lattice potential is then suddenly shut off; (b) absorption images of multiple matter wave interference patterns after 30-ms time of flight; (c) total atom numbers of (b) versus lattice depth.

remains in the many body ground states of the system. Then by adiabatically ramping down the lattice potential, the BEC should be recovered. For example, we loaded a BEC in a 1D system. The lattice depth was ramped up to 14 E_R in 40 ms. After a hold time of 90 ms, the lattice potential was ramped down to 0 E_R (see Fig. 3(a)). The lattice lifetime is highly sensitive to slight intensity fluctuations in the lattice beams. Absorption images are taken after free expansion of 30 ms. Comparing the absorption images of the BEC (see Fig. 3(b)) and the one that undergoes the reversible loading process (see Fig. 3(c)), we found that this power control system does not heat the condensate.

If a lattice potential is adiabatically ramped up to a large potential depth, atoms undergo trap states from the coherent superfluid state to the incoherent number squeezed state. We ramped the lattice to different optical depths in 40 ms. After a hold time of 50 ms, the lattice potential suddenly switched off (see Fig. 4(a)). At low lattice depths, the BEC atoms can be described as a giant macroscopic matter wave. When such a condensate is released from the trapping potential, a multiple matter-wave interference pattern can be seen, owing to the phase coherence between the atomic wave functions on different lattice sites. At deep lattice depths, the system tends to become a system where the number of atoms is fixed at each lattice site, which can be referred to as atomic squeezing[17]. Tunneling is also suppressed so that phase coherence between sites is lost and no matter-wave interference can be seen when the quantum gases are released from the lattice potential. Absorption images are taken after free expansion of 30 ms (see Fig. 4(b)). In addition, the total atom numbers measured versus the lattice depth show no loss of atoms (see Fig. 4(c)). These experimental results show that the power control system does not heat the atoms and works well for optical lattice experiments.

In conclusion, we present an effective laser power control system. Some essential points used for optimizing the performance are discussed. A RF modulator, a fast photodetector, and an angle-polished fiber are employed. We set up the AOM in a new way and optimize the time sequence for it. As a result, a large-scale (0–160 E_R), low noise (0.3%), and highly stabilized power control system with a response time shorter than 20 μs is achieved. We perform primary optical lattice experiments as examples to show that this power control system is sufficient for experiments. With these performances, our power control system can be of great interest in cold atom physics, precision measurements, and for applications requiring controllable optical sources.

This work was partially supported by the National "973" Program of China (No. 2011CB921501) and the National Natural Science Foundation of China (Nos. 61027016, 61078026, 10874008, and 10934010).

References

1. M. Takamoto, F. Hong, R. Higashi, and H. Katori, Nature **435,** 321 (2005).
2. I. Bloch, Nature **453,** 1016 (2008).
3. M. Greiner, O. Mandel, T. Esslinger, T. Hänsch, and I. Bloch, Nature **415,** 39 (2002).
4. X. Zhou, X. Xu, L. Yin, W. Liu, and X. Chen, Opt. Express **18,** 15664 (2010).
5. H. Pu, W. Zhang, and P. Meystre, Phys. Rev. Lett. **87,** 140405 (2001).
6. E. Demler and F. Zhou, Phys. Rev. Lett. **88,** 163001 (2002).
7. T. Schulte, S. Drenkelforth, J. Kruse, W. Ertmer, J. Arlt, K. Sacha, J. Zakrzewski, and M. Lewenstein, Phys. Rev. Lett. **95,** 170411 (2005).
8. R. Grimm, M. Weidemüller, and Y. Ovchinnikov, Adv. Atom Mol. Opt. Phys. **42,** 95 (2000).
9. D. Xiong, P. Wang, Z. Fu, S. Chai, and J. Zhang, Chin. Opt. Lett. **8,** 627 (2010).
10. R. Drever, J. Hall, F. Kowalski, J. Hough, G. Ford, A. Munley, and H. Ward, Applied Physics B **31,** 97 (1983).
11. F. Yang, X. Zhou, J. Li, Y. Chen, L. Xia, and X. Chen, Phys. Rev. A **78,** 043611 (2008).
12. X. Zhou, F. Yang, X. Yue, T. Vogt, and X. Chen, Phys. Rev. A **81,** 013615 (2010).
13. T. Zhou, X. Chen, Qi, Q. Wang, W. Xiong, J. Duan, X. Zhou, and X. Chen, Chin. Opt. Lett. **8,** 496 (2010).
14. Q. Ma, L. Xia, B. Lu, W. Xiong, Y. Zhang, X. Zhou, and X. Chen, Chin. Opt. Lett. **7,** 46 (2009).
15. R. Sapiro, R. Zhang, and G. Raithel, New J. Phys. **11,** 013013 (2009).
16. H. Chen, D. Xiong, P. Wang, and J. Zhang, Chin. Opt. Lett. **8,** 348 (2010).
17. C. Orzel, A. Tuchman, M. Fenselau, M. Yasuda, and M. Kasevich, Science **291,** 2386 (2001).